

ENERGY-INSPIRED FLIGHT CONTROL WITH FORMAL GUARANTEES

Ian J. Willebeek-LeMair* and Craig A. Woolsey†

Virginia Tech, Blacksburg, VA 24061

April 22, 2025

Abstract

This paper reviews recent results related to robust model-based inertial position tracking for small air vehicles. The control law discussed is formulated in an energy-based modeling framework and the closed-loop system is robust with respect to disturbances. Specific formal guarantees are stated. The main contribution of this paper is a discussion regarding the use of the formal guarantees for control tuning. Simulations are used to demonstrate the tuning approach and the robust behavior.

1 Introduction

Right now, the aerospace industry, the FAA, and NASA are working together to build a future they call Advanced Air Mobility (AAM). NASA’s vision is to make aviation accessible everywhere and to integrate it into transportation and shipping systems at the national, regional, and local levels [1]. A central theme of this work is ensuring safety. As AAM matures, unmanned aircraft systems (UAS) will need to operate with control systems that are robust to disturbances and model uncertainty. One approach that may fill this gap is to require flight controllers that provide formal guarantees.

To achieve the level of safety needed for widespread integration of UAS into the nation’s infrastructure, UAS must operate in a manner that is certifiably safe even in uncertain environments. This includes inclement weather and the kind of heavy turbulence and strong wind fields that may be found in urban canyons. Traditional modeling of aircraft is largely limited to linear models. These models are only valid locally and there is no formal method for specifying the region in which the linear approximation is valid. To evaluate the safety of UAS operating in uncertain environments, sophisticated nonlinear methods are needed. Real aircraft are nonlinear, so well-developed nonlinear models are typically valid over a much larger envelope than their linear counterparts.

Recently, the authors have proposed a robust nonlinear model-based energy-inspired inertial position tracking controller that applies to a large class of air systems. This controller is outfitted with formal guarantees that can be used to certify safety. The formal guarantees bound the difference between the aircraft’s intended position and its actual position. The bound is stated in terms of disturbances affecting the system. These disturbances capture both exogenous effects like gusts and other sources of uncertainty such as modeling error.

The main contributions of the present work are twofold. Some of the most common AAM platforms are multirotors. Accordingly, the first contribution of this work is to summarize the results of [2] and specify them to the case of a multirotor aircraft. Next, an enduring challenge faced by nonlinear control methods is that they can be difficult to understand and challenging to tune. The second contribution of this work is to detail a principled approach to tuning the proposed nonlinear controller that draws on the intuitive notion of energy.

The paper is organized as follows. Section 2 details the aircraft model considered in this work. Section 3 discusses the recently proposed inertial position tracking controller. Section 4 proposes a principled approach to tuning that leverages the controller’s formal guarantees. Section 5 reviews a simulation that demonstrates the tuned performance. Finally, section 6 offers conclusions.

2 Aircraft Model

Consider a rigid multirotor aircraft that produces thrust along an axis fixed in the body. Let $\{\mathbf{i}_1, \mathbf{i}_2, \mathbf{i}_3\}$ denote an inertial North-East-Down reference frame, \mathcal{F}_i , fixed to the surface of the Earth and let $\{\mathbf{b}_1, \mathbf{b}_2, \mathbf{b}_3\}$ denote a body-fixed reference frame,

Copyright ©2025 by Ian Willebeek-LeMair. Reproduced by the Virginia Space Grant Consortium with permission. All rights reserved.

*Ph.D. Student, Kevin T. Crofton Department of Aerospace and Ocean Engineering, ianwl@vt.edu

†Professor, Kevin T. Crofton Department of Aerospace and Ocean Engineering, cwoolsey@vt.edu

\mathcal{F}_b , located at the vehicle's center of mass. Let \mathbf{b}_1 point along the longitudinal axis of the aircraft, \mathbf{b}_2 along the lateral axis, and \mathbf{b}_3 along the directional axis. Suppose that the vehicle produces propulsive force along $\mathbf{b}_T = -\mathbf{b}_3$. The reference frames are illustrated in Figure 1.

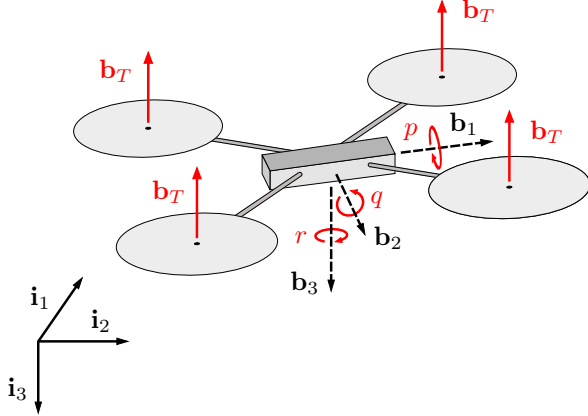


Figure 1: Selected reference frames.

Let the position of the vehicle's center of mass with respect to \mathcal{F}_i be denoted $\mathbf{r} = [x \ y \ z]^T$. Let the attitude of the vehicle be represented by the unit quaternion $\mathbf{q} = [q_0 \ \bar{\mathbf{q}}^T]^T \in S^3$. The proper rotation matrix that corresponds to \mathbf{q} and maps free vectors in \mathcal{F}_b to those in \mathcal{F}_i is

$$\mathbf{R}(\mathbf{q}) = (q_0^2 - \|\bar{\mathbf{q}}\|^2)\mathbf{I} + 2\bar{\mathbf{q}}\bar{\mathbf{q}}^T + 2q_0\hat{\mathbf{q}} \quad (1)$$

where $\hat{(\cdot)}$, sometimes denoted $(\cdot)^\wedge$, is the cross product equivalent matrix operator defined by the identity $\hat{\mathbf{a}}\mathbf{b} = \mathbf{a} \times \mathbf{b}$ for all $\mathbf{a}, \mathbf{b} \in \mathbb{R}^3$. Note that $\hat{\mathbf{a}} \in \mathbb{R}^{3 \times 3}$ is skew symmetric: $(\hat{\mathbf{a}})^T = -\hat{\mathbf{a}}$.

Let $\mathbf{v} = [u \ v \ w]^T$ denote the velocity of the body with respect to \mathcal{F}_i , expressed in \mathcal{F}_b . Let $\boldsymbol{\omega} = [p \ q \ r]^T$ denote the angular velocity of \mathcal{F}_b with respect to \mathcal{F}_i , expressed in \mathcal{F}_b .

The vehicle experiences four forces: gravitational force, $mg\mathbf{R}(\mathbf{q})^T\mathbf{e}_3$; aerodynamic force, \mathbf{a}_f ; propulsive force $u_T\mathbf{e}_T$; and disturbance force \mathbf{w}_f . For control design purposes, we use the aerodynamic model

$$\mathbf{a}_f(\mathbf{v}) = -\frac{1}{2}\rho SC_D \|\mathbf{v}\| \mathbf{v} \quad (2)$$

where ρ is the local air density, S is a reference area, and C_D is the vehicle's (constant) coefficient of drag. The propulsive force $u_T\mathbf{e}_T$ is the product of the thrust intensity u_T and the unit vector along which thrust acts, which is $\mathbf{e}_T = -\mathbf{e}_3$ when resolved in the coordinates of the body frame. The disturbance force \mathbf{w}_f captures the difference between the forces experienced by the real vehicle and those that are otherwise

modeled. For example, the aerodynamic force model used in the control design process and the model used in the simulations of Section 5 are different. Therefore, for the purpose of the formal guarantees, the difference of these two models is lumped into \mathbf{w}_f .

In this work, we suppose that an inner-loop controller controls the angular velocity of the vehicle. We therefore model the angular velocity as $\boldsymbol{\omega} = \mathbf{u}_\omega + \mathbf{w}_\omega$ where \mathbf{u}_ω is the angular velocity command to the inner-loop controller and \mathbf{w}_ω is the difference between the vehicle's angular velocity and the commanded angular velocity that arises from imperfect tracking. For the sake of the following analysis, \mathbf{u}_ω is regarded as a control input and \mathbf{w}_ω is regarded as a disturbance.

With the established definitions, the differential equations governing the aircraft system are

$$\begin{aligned} \dot{\mathbf{r}} &= \mathbf{R}(\mathbf{q})\mathbf{v} \\ \dot{\mathbf{v}} &= \mathbf{v} \times (\mathbf{u}_\omega + \mathbf{w}_\omega) + g\mathbf{R}(\mathbf{q})^T\mathbf{e}_3 \\ &\quad + \frac{1}{m}\mathbf{a}_f(\mathbf{v}) + \frac{1}{m}u_T\mathbf{e}_T + \frac{1}{m}\mathbf{w}_f \\ \dot{\mathbf{q}} &= E(\mathbf{q})(\mathbf{u}_\omega + \mathbf{w}_\omega) \end{aligned} \quad (3)$$

where $E(\mathbf{q}) = \frac{1}{2}[-\bar{\mathbf{q}} \ q_0\mathbf{I} - \hat{\bar{\mathbf{q}}}]^T$ and m is the mass of the aircraft. The input to this system is $\mathbf{u} = [u_T \ \mathbf{u}_\omega^T]^T$ and the disturbance is $\mathbf{w} = [\mathbf{w}_f^T \ \mathbf{w}_\omega^T]^T$.

3 Position Tracking Controller

In [2], the authors developed a nonlinear position tracking flight control law with stability guarantees. Due to page limits, it is not practical to present the complete derivation of the controller. Instead, the control law, with specialization to the aerodynamic model (2), is detailed in the [appendix](#).

The controller is an output tracking controller that drives the vehicle to follow a user specified path $\mathbf{r}^* : [t_0, \infty) \rightarrow \mathbb{R}^3$ while pointing its longitudinal axis in a user specified direction $\boldsymbol{\eta} : [t_0, \infty) \rightarrow \mathbb{R}^3$. In [2], the output tracking problem is defined in terms of the state of the vehicle $\mathbf{x} = [\mathbf{r}^T \ \mathbf{v}^T \ \mathbf{q}^T]^T$, a target state $\mathbf{x}^* = [\mathbf{r}^{*T} \ \mathbf{v}^{*T} \ \mathbf{q}^{*T}]^T \in \mathbb{R}^3 \times \mathbb{R}^3 \times S^3$, and an error vector $\boldsymbol{\xi} = [\boldsymbol{\xi}_1^T \ \boldsymbol{\xi}_2^T \ \boldsymbol{\xi}_3^T]^T \in \mathbb{R}^3 \times \mathbb{R}^3 \times \mathcal{B}^3$. These three quantities are defined such that

$$\begin{aligned} \boldsymbol{\xi}_1 = \mathbf{0} &\Leftrightarrow \mathbf{r} = \mathbf{r}^* \\ \boldsymbol{\xi}_2 = \mathbf{0} &\Leftrightarrow \mathbf{v} = \mathbf{v}^* \\ \boldsymbol{\xi}_3 = \mathbf{0} &\Leftrightarrow \mathbf{R}(\mathbf{q}) = \mathbf{R}(\mathbf{q}^*) \end{aligned} \quad (4)$$

Therefore, the vehicle is perfectly tracking the prescribed position history when $\boldsymbol{\xi} = \mathbf{0}$. In particular, the error vectors are defined as

$$\boldsymbol{\xi}_1 = \mathbf{r} - \mathbf{r}^* \quad (5)$$

$$\boldsymbol{\xi}_2 = \frac{1}{m}\mathbf{P}_{22}^{-1}\mathbf{R}(\mathbf{q})(\mathbf{v} - \mathbf{v}^*) \quad (6)$$

$$\boldsymbol{\xi}_3 = 2E(\mathbf{q})^T\mathbf{q}^* \quad (7)$$

The formulation of the controller described in the [appendix](#) involves a number of tuning parameters. These are the scalars $\theta \in (0, 1)$ and $P_{33}, \beta, \mu_f, \mu_\omega \in \mathbb{R}$ and the matrices $\mathbf{P}_{11}, \mathbf{P}_{22}, \mathbf{K}_{11}, \mathbf{K}_{22}, \mathbf{K}_{33} \in \mathbb{R}^{3 \times 3}$. Note, these five matrices are all symmetric.

Consider the positive definite function $V : \mathbb{R}^3 \times \mathbb{R}^3 \times \bar{\mathcal{B}}^3 \rightarrow \mathbb{R}$ defined by

$$V(\boldsymbol{\xi}) = \frac{1}{2} \boldsymbol{\xi}_1^\top \mathbf{P}_{11} \boldsymbol{\xi}_1 + \frac{1}{2} \boldsymbol{\xi}_2^\top \mathbf{P}_{11} \boldsymbol{\xi}_2 + P_{33} (1 - \sqrt{1 - \|\boldsymbol{\xi}_3\|^2}) \quad (8)$$

In [2] this function represents a notion of error energy for the closed-loop system. Each term is the error energy associated with the corresponding error vector. The position error energy, $V_1(\boldsymbol{\xi}_1) = \frac{1}{2} \boldsymbol{\xi}_1^\top \mathbf{P}_{11} \boldsymbol{\xi}_1$ and the velocity error energy $V_2(\boldsymbol{\xi}_2) = \frac{1}{2} \boldsymbol{\xi}_2^\top \mathbf{P}_{22} \boldsymbol{\xi}_2$ are quadratic. The attitude error energy $V_3(\boldsymbol{\xi}_3) = P_{33} (1 - \sqrt{1 - \|\boldsymbol{\xi}_3\|^2})$ is not quadratic because $\boldsymbol{\xi}_3$ lives in $\bar{\mathcal{B}}^3$, not \mathbb{R}^3 . Unlike $V_1(\boldsymbol{\xi}_1)$ and $V_2(\boldsymbol{\xi}_2)$, the error energy function $V_3(\boldsymbol{\xi}_3)$ is bounded on its domain. This property is practical in the following sense. While it is implausible that a physical disturbance would drive either position or velocity to infinity in finite time, it is plausible that a disturbance might drive a vehicle to 180° of attitude error in finite time. Therefore, we do not want this most extreme attitude error to be penalized as much as infinite position or velocity error. Accordingly, 180° of attitude error corresponds to a finite amount of error energy.

For the following analysis, we prescribe $\mathbf{K}_{11} = \frac{1}{2} k_1 \mathbf{P}_{11}^{-1}$, $\mathbf{K}_{22} = \frac{1}{2} k_2 \mathbf{P}_{22}^{-1}$, and $\mathbf{K}_{33} = k_3 P_{33}^{-1} \mathbf{I}$. Then, analysis presented in [2] shows that the rate of change of V along trajectories of the closed-loop system is bounded by

$$\begin{aligned} \dot{V}(t, \boldsymbol{\xi}, \mathbf{w}) &\leq -k_1 V_1(\boldsymbol{\xi}_1) - k_2 V_2(\boldsymbol{\xi}_2) - k_3 V_3(\boldsymbol{\xi}_3) \\ &\quad + \beta \left(\frac{1}{2} \left\| \frac{\mathbf{w}_f}{\mu_f} \right\|^2 + \frac{1}{2} \left\| \frac{\mathbf{w}_\omega}{\mu_\omega} \right\|^2 \right) \end{aligned} \quad (9)$$

In the next section, we discuss and study how (8) and (9) can be used for control tuning. Before discussing tuning, however, we note the formal guarantee that results from (8) and (9).

Take $\kappa = \min\{k_1, k_2, k_3\}$ and $b = \min\{\frac{\beta}{2\mu_f^2}, \frac{\beta}{2\mu_\omega^2}\}$. Then (9) implies that

$$\dot{V}(t, \boldsymbol{\xi}, \mathbf{w}) \leq -\kappa V(\boldsymbol{\xi}) + b \|\mathbf{w}\|_\infty^2 \quad (10)$$

Hence, applying the Comparison Lemma [3] results in

$$V(\boldsymbol{\xi}(t)) \leq e^{-\kappa(t-t_0)} V(\boldsymbol{\xi}(t_0)) + \frac{b}{\kappa} (1 - e^{-\kappa(t-t_0)}) \|\mathbf{w}\|_\infty^2 \quad (11)$$

This inequality is a formal guarantee describing how error evolves in the system. $V(\boldsymbol{\xi})$ describes the

amount of error present in the system. Hence, (11) states that the error energy decays exponentially to the ultimate bound $\frac{b}{\kappa} \|\mathbf{w}\|_\infty^2$. Consequently, the error vector $\boldsymbol{\xi}$ decays asymptotically to its own ultimate bound. This formal guarantee is a tool that designers can use to ensure safe and predictable flight.

4 Controller Tuning

This section details physics-inspired insights that can be used for tuning the proposed controller.

Consider equation (8) and the parameters \mathbf{P}_{11} , \mathbf{P}_{22} , and P_{33} . The function V is error energy that the closed-loop system will dissipate. The parameters \mathbf{P}_{11} , \mathbf{P}_{22} , and P_{33} govern the relative weight attributed to position, velocity, and attitude error. These weights can be tailored to control the manner in which the system dissipates error. For example, if \mathbf{P}_{11} is selected to be much larger than both \mathbf{P}_{22} and P_{33} , then the closed-loop system is permitted to decrease overall error by converting position error $\boldsymbol{\xi}_1$ into velocity error $\boldsymbol{\xi}_2$ and attitude error $\boldsymbol{\xi}_3$. Conversely, if P_{33} is selected to be much larger than \mathbf{P}_{11} and \mathbf{P}_{22} , then the closed-loop system will only permit small amounts of attitude error $\boldsymbol{\xi}_3$ as it decreases overall error V .

In the view of the authors, the best practice for tuning \mathbf{P}_{11} , \mathbf{P}_{22} , and P_{33} is similar to an approach commonly used to tune linear quadratic regulators. In particular, the approach is to identify soft maximum tolerable position, velocity, and attitude errors Δr_{\max} , Δv_{\max} , and $\Delta \Phi_{\max}$ and to prescribe \mathbf{P}_{11} , \mathbf{P}_{22} , and P_{33} so that each of these conditions correspond to equivalent error energies. The following discussion elaborates on this idea.

To discuss the notion of a maximum tolerable angular offset $\Delta \Phi_{\max}$, recall the Euler axis-angle formalism for rotations. The Euler axis $\mathbf{a} \in S^2$, Euler angle $\Phi \in [0, \pi]$, and corresponding rotation matrix \mathbf{R} are related by

$$\mathbf{R} = e^{\Phi \hat{\mathbf{a}}}, \quad \Phi = \cos^{-1}\left(\frac{\text{tr} \mathbf{R} - 1}{2}\right), \quad \hat{\mathbf{a}} = \frac{\mathbf{R} - \mathbf{R}^\top}{2 \sin \Phi} \quad (12)$$

This formalism views the rotation \mathbf{R} as a rotation by the angle Φ about the axis defined by the unit vector \mathbf{a} . Consider the angle $\Delta \Phi$ between the vehicle attitude \mathbf{q} and the target attitude \mathbf{q}^* . It can be shown that

$$\cos(\Delta \Phi) = \frac{\text{tr}(\mathbf{R}(\mathbf{q})^\top \mathbf{R}(\mathbf{q}^*)) - 1}{2} = 1 - 2 \|\boldsymbol{\xi}_3\|^2 \quad (13)$$

where the first equality is the definition of the Euler angle $\Delta \Phi$ and the second results from algebraic manipulations. It follows from (13) that $\Delta \Phi = \Delta \Phi_{\max}$ if and only if

$$\|\boldsymbol{\xi}_3\|^2 = \frac{1}{2} (1 - \cos(\Delta \Phi_{\max})) \quad (14)$$

Next, we select \mathbf{P}_{11} , \mathbf{P}_{22} , and P_{33} so that all of the soft maximums correspond to the same error energies

$$\begin{aligned} \|\mathbf{r} - \mathbf{r}^*\| = \Delta r_{\max} &\Leftrightarrow V_1(\boldsymbol{\xi}_1) = 1 \\ \|\mathbf{v} - \mathbf{v}^*\| = \Delta v_{\max} &\Leftrightarrow V_2(\boldsymbol{\xi}_2) = 1 \\ \Delta\Phi = \Delta\Phi_{\max} &\Leftrightarrow V_3(\boldsymbol{\xi}_3) = 1 \end{aligned} \quad (15)$$

This objective is achieved by the prescriptions

$$\mathbf{P}_{11} = 2(\Delta r_{\max})^{-2}\mathbf{I} \quad (16)$$

$$\mathbf{P}_{22} = 2(\Delta v_{\max}/m)^2\mathbf{I} \quad (17)$$

$$P_{33} = \left(1 - \sqrt{\frac{1}{2}(1 - \cos(\Delta\Phi_{\max}))}\right)^{-1} \quad (18)$$

With the parameters \mathbf{P}_{11} , \mathbf{P}_{22} , and P_{33} prescribed, we now turn to tuning μ_f , μ_ω , k_1 , k_2 , k_3 , and β based on (9).

In (9), the parameters μ_f and μ_ω play roles analogous to those of \mathbf{P}_{11} , \mathbf{P}_{22} , and P_{33} in (8). To normalize the effects of the disturbances \mathbf{w}_f and \mathbf{w}_ω , we select μ_f and μ_ω to be equal to the soft maximum amplitudes of disturbances that we expect the system to experience. Identifying these soft maximums as $\mathbf{w}_{f,\max}$ and $\mathbf{w}_{\omega,\max}$, we prescribe

$$\mu_f = \mathbf{w}_{f,\max} \quad \text{and} \quad \mu_\omega = \mathbf{w}_{\omega,\max} \quad (19)$$

Furthermore, we define the function L by

$$L(\mathbf{w}) = \frac{1}{2} \left\| \frac{\mathbf{w}_f}{\mathbf{w}_{f,\max}} \right\|^2 + \frac{1}{2} \left\| \frac{\mathbf{w}_\omega}{\mathbf{w}_{\omega,\max}} \right\|^2 \quad (20)$$

With these prescriptions and definitions, (9) is now

$$\dot{V}(t, \boldsymbol{\xi}, \mathbf{w}) \leq -k_1 V_1(\boldsymbol{\xi}_1) - k_2 V_2(\boldsymbol{\xi}_2) - k_3 V_3(\boldsymbol{\xi}_3) + \beta L(\mathbf{w}) \quad (21)$$

The right hand side of this equation is a linear combination of terms whose value is nominally zero and whose value is equal to one when the system is at the corresponding soft maximum.

The inequality (21) can be further simplified by taking $k_1, k_2, k_3 = k$ for some $k > 0$. In this case, (21) becomes

$$\dot{V}(t, \boldsymbol{\xi}, \mathbf{w}) \leq -kV(\boldsymbol{\xi}) + \beta L(\mathbf{w}) \quad (22)$$

This resembles a standard first order linear time-invariant differential equation, so the roles played by k and β can be readily interpreted. The term k defines the responsiveness of the system. When k is large, the system will settle to equilibrium quickly. When k is small, the system will settle slowly. Larger values of k typically correspond to larger control efforts and likewise for smaller values. The term β

governs the sensitivity of the equilibrium error condition to disturbances. When the ratio β/k is large, the equilibrium error is highly sensitive to disturbances. When the ratio β/k is small, the equilibrium error is insensitive. Larger values of β/k correspond to lower levels of control effort—the system permits more error and so is using less control effort to counteract error. Smaller values of β/k correspond to higher levels of control effort—the system permits less error and so the controller must use substantial control effort to counteract error.

While the prescription $k_1, k_2, k_3 = k$ does simplify the guarantee (21), retaining distinct values for k_1 , k_2 , and k_3 is beneficial. Using distinct values for these terms enables the designer to tailor the rate at which each type of error is dissipated from the system. In particular, choosing $k_3 > k_2 > k_1$ sets up a hierarchy of time scales so that the aircraft eliminates attitude error first, then velocity error, then position error. This order resembles how a human pilot might fly and therefore makes the control law behave more predictably.

5 Simulation

To demonstrate the controller with the discussed tuning strategy, a simulated flight of a multirotor aircraft is presented. The position history of the aircraft is illustrated in Figure 2. The time histories of the disturbances \mathbf{w}_f and \mathbf{w}_ω are pictured in Figure 3 and Figure 4, respectively. The input history resulting from the controller is shown in Figure 5. Finally, the path that vehicle takes through 3-dimensional space is illustrated in Figure 6.

The control law is tuned according to the method described in Section 4. The selected values of the tuning parameters are noted in Table 1.

Table 1: Controller parameters.

Δr_{\max}	1 m	k_1	2 Hz
Δv_{\max}	1 m/s	k_2	4 Hz
$\Delta\Phi_{\max}$	$\pi/9$ rad	k_3	20 Hz
μ_f	1 N	β	1
μ_ω	1 rad/s	θ	0.1

In the simulation, the aerodynamics of the vehicle are governed by the model presented in [4], which uses data from the wind tunnel tests discussed in [5]. The aerodynamic model used for control design, however, is that of (2). Accordingly, the difference in the aerodynamic force of these two models is, from the perspective of the control law, the disturbance force \mathbf{w}_f .

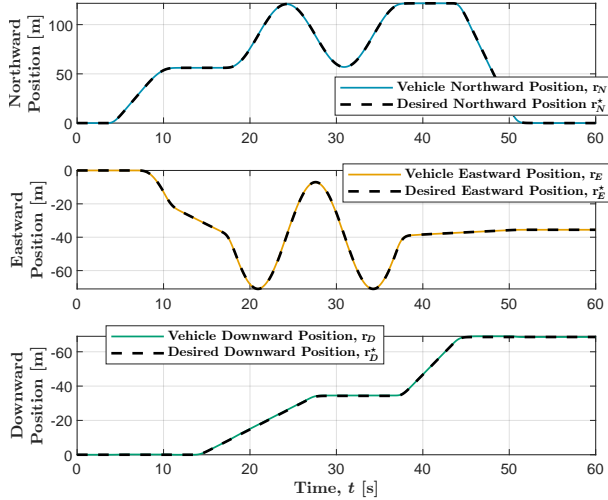


Figure 2: Vehicle position history

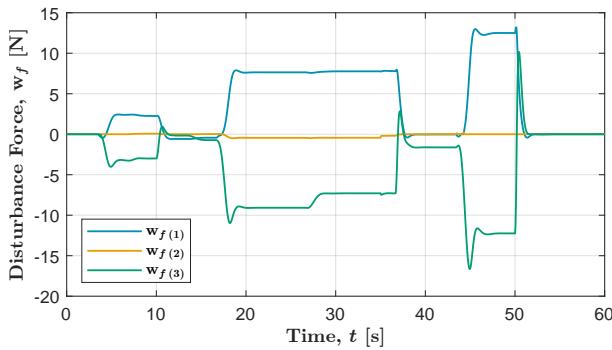


Figure 3: Disturbance force history

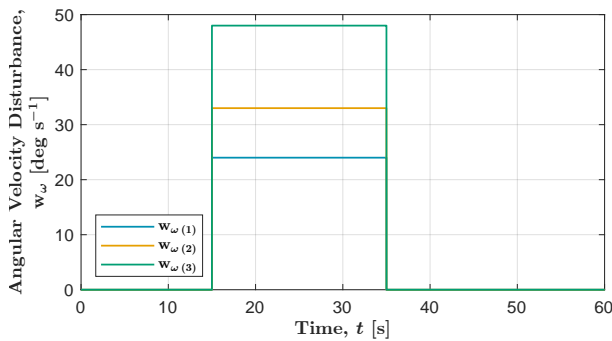


Figure 4: Disturbance angular velocity history

6 Conclusions

This paper has detailed a robust position-tracking flight controller and discussed its application to multirotor aircraft. A special case of the controller formulation for a quadratic drag model was identified. The controller's formal guarantees were identified and discussed. A principled approach to tuning the controller that leveraged the formal guarantees was dis-

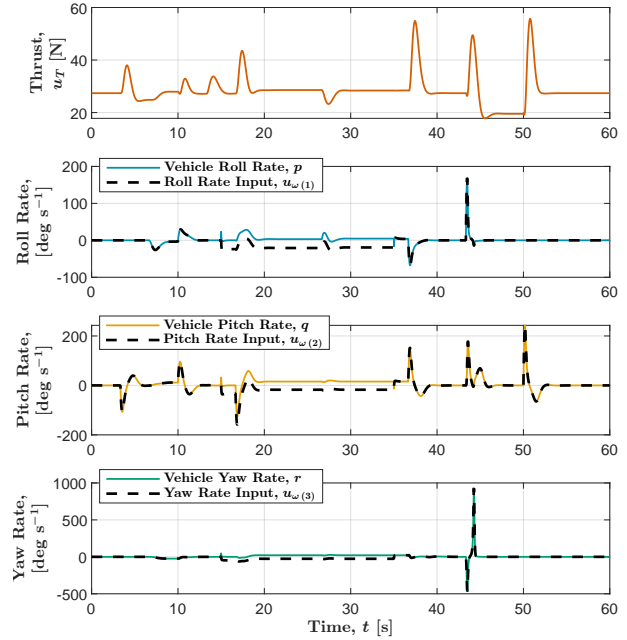


Figure 5: Control input history

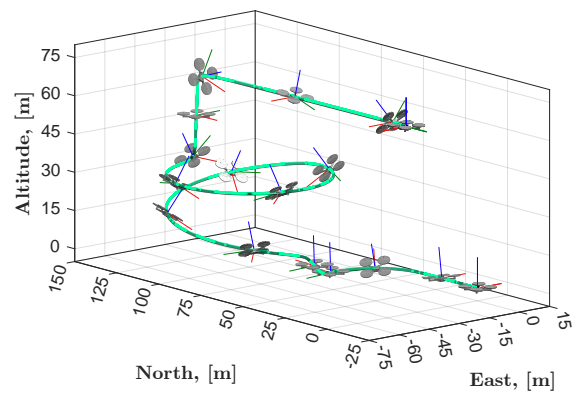


Figure 6: Vehicle flight path

cussed in detail and specific recommendations were made. The proposed approach to tuning was demonstrated in simulation.

Acknowledgments

The first author gratefully acknowledges the support of the Virginia Space Grant Consortium under the graduate research fellowship.

Appendix: Control Law Specification

This appendix presents the equations that comprise the control law discussed in Section 3. This controller was developed in [2] and is restated here for completeness. Due to page limits, this appendix contains no discussion and simply states relevant equa-

tions. For a complete discussion, see [2].

The controller is

$$\begin{aligned} u_T &= (1 - 2\|\bar{\varepsilon}\|^2)\|\mathbf{T}^*\| \\ \boldsymbol{\omega} &= (\mathbf{I} - \Psi_\omega)^{-1}(\boldsymbol{\omega}_0^* + \boldsymbol{\omega}_{\mathcal{J}} + \boldsymbol{\omega}_{\mathcal{R}}) \end{aligned} \quad (23)$$

Before defining all of the terms in (23), note that Ψ_ω simplifies dramatically for the selected control-design aerodynamic model (2). Ψ_ω is defined as

$$\begin{aligned} \Psi_\omega &= \frac{1}{\|\mathbf{T}^*\|} \left(\frac{\boldsymbol{\sigma}^\top \boldsymbol{\lambda}}{\|\boldsymbol{\sigma} \times \boldsymbol{\lambda}\|} \mathbf{e}_T \mathbf{e}_2^\top + \hat{\mathbf{e}}_T \right) \\ &\quad \cdot \mathbf{R}(\boldsymbol{\varepsilon})^\top \left(\hat{\mathbf{a}}_f(\mathbf{v}) - \frac{\partial \mathbf{a}_f(\mathbf{v})}{\partial \mathbf{v}} \hat{\mathbf{v}} \right) \end{aligned} \quad (24)$$

For the aerodynamic model (2), the last factor on the right hand side of (24) simplifies to

$$\begin{aligned} \hat{\mathbf{a}}_f(\mathbf{v}) - \frac{\partial \mathbf{a}_f(\mathbf{v})}{\partial \mathbf{v}} \hat{\mathbf{v}} &= -\frac{1}{2} \rho S C_D \|\mathbf{v}\| \hat{\mathbf{v}} + \frac{1}{2} \rho S C_D \left(\|\mathbf{v}\| \mathbf{I} + \frac{\mathbf{v} \mathbf{v}^\top}{\|\mathbf{v}\|} \right) \hat{\mathbf{v}} \\ &= -\frac{1}{2} \rho S C_D \left(\|\mathbf{v}\| \hat{\mathbf{v}} - \|\mathbf{v}\| \hat{\mathbf{v}} \right) = \mathbf{0} \end{aligned}$$

and, hence, $\Psi_\omega = \mathbf{0}$. The controller is, therefore,

$$\begin{aligned} u_T &= (1 - 2\|\bar{\varepsilon}\|^2)\|\mathbf{T}^*\| \\ \boldsymbol{\omega} &= \boldsymbol{\omega}_0^* + \boldsymbol{\omega}_{\mathcal{J}} + \boldsymbol{\omega}_{\mathcal{R}} \end{aligned} \quad (25)$$

The terms appearing in (25) are defined as follows. The feedforward angular velocity $\boldsymbol{\omega}_0^*$ is

$$\begin{aligned} \boldsymbol{\omega}_0^* &= -k_\eta \mathbf{e}_T (\boldsymbol{\sigma} \times \boldsymbol{\lambda})^\top \boldsymbol{\eta} \\ &\quad + \frac{1}{\|\mathbf{T}^*\|} \left(\frac{\boldsymbol{\sigma}^\top \boldsymbol{\lambda}}{\|\boldsymbol{\sigma} \times \boldsymbol{\lambda}\|} \mathbf{e}_T (\boldsymbol{\chi} \times \boldsymbol{\lambda})^\top + \hat{\mathbf{e}}_T \mathbf{R}(\mathbf{q}^*)^\top \right) \dot{\mathbf{T}}_0^* \end{aligned} \quad (26)$$

The interconnection angular velocity $\boldsymbol{\omega}_{\mathcal{J}}$ is

$$\boldsymbol{\omega}_{\mathcal{J}} = -\frac{4\|\mathbf{T}^*\|}{mP_{33}} \operatorname{sgn}(\varepsilon_0) ((\mathbf{e}_T^\top \bar{\boldsymbol{\varepsilon}}) \mathbf{I} + \varepsilon_0 \hat{\mathbf{e}}_T) \mathbf{R}(\mathbf{q})^\top \boldsymbol{\xi}_2 \quad (27)$$

The dissipation angular velocity $\boldsymbol{\omega}_{\mathcal{R}}$ is

$$\boldsymbol{\omega}_{\mathcal{R}} = 2 \operatorname{sgn}(\varepsilon_0) \tilde{\mathcal{R}}_{33} P_{33} \bar{\boldsymbol{\varepsilon}} \quad (28)$$

The dissipation matrix $\tilde{\mathcal{R}}_{33}$ is

$$\tilde{\mathcal{R}}_{33} = \left(\mathbf{K}_{33} + \left(\frac{1}{8} \frac{\mu_f^2}{\theta \beta} \right) \Psi_f \Psi_f^\top + \left(\frac{1}{8} \frac{\mu_\omega^2}{\beta} \right) \mathbf{I} \right) \quad (29)$$

where Ψ_f is defined by

$$\begin{aligned} \Psi_f &= \frac{1}{\|\mathbf{T}^*\|} \left(\frac{\boldsymbol{\sigma}^\top \boldsymbol{\lambda}}{\|\boldsymbol{\sigma} \times \boldsymbol{\lambda}\|} \mathbf{e}_T (\boldsymbol{\chi} \times \boldsymbol{\lambda})^\top \right. \\ &\quad \left. + \hat{\mathbf{e}}_T \mathbf{R}(\mathbf{q}^*)^\top \right) \left(-\frac{1}{m} \mathbf{R}(\mathbf{q}) \frac{\partial \mathbf{a}_f(\mathbf{v})}{\partial \mathbf{v}} \right. \\ &\quad \left. - (\mathbf{K}_{11} \mathbf{P}_{11} + \mathbf{P}_{22} \mathcal{R}_{22}) \mathbf{R}(\mathbf{q}) \right) \end{aligned} \quad (30)$$

The disturbance free rate of the target thrust is

$$\begin{aligned} \dot{\mathbf{T}}_0^* &= -\mathbf{R}(\mathbf{q}) \frac{\partial \mathbf{a}_f(\mathbf{v})}{\partial \mathbf{v}} \left(g \mathbf{R}(\mathbf{q})^\top \mathbf{e}_3 + \frac{1}{m} \mathbf{a}_f(\mathbf{v}) + \frac{1}{m} \mathbf{e}_T u_T \right) \\ &\quad + m \left((\mathbf{K}_{11} \mathbf{P}_{11})^2 - \mathbf{P}_{22} \mathbf{P}_{11} \right) (-\mathbf{K}_{11} \mathbf{P}_{11} \boldsymbol{\xi}_1 + \mathbf{P}_{22} \boldsymbol{\xi}_2) \\ &\quad - (\mathbf{K}_{11} \mathbf{P}_{11} + \mathbf{P}_{22} \mathcal{R}_{22}) (m g \mathbf{e}_3 + \mathbf{R}(\mathbf{q}) \mathbf{a}_f(\mathbf{v})) \\ &\quad + \mathbf{R}(\mathbf{q}) \mathbf{e}_T u_T - m \dot{\mathbf{r}}^* + m \mathbf{K}_{11} \mathbf{P}_{11} (-\mathbf{K}_{11} \mathbf{P}_{11} \boldsymbol{\xi}_1 \\ &\quad + \mathbf{P}_{22} \boldsymbol{\xi}_2) + m \dot{\mathbf{r}}^* \end{aligned} \quad (31)$$

The dissipation matrix \mathcal{R}_{22} is

$$\mathcal{R}_{22} = \mathbf{K}_{22} + \left(\frac{1}{2} \frac{1}{m^2} \frac{\mu_f^2}{(1-\theta)\beta} \right) \mathbf{P}_{22}^{-2} \quad (32)$$

The attitude error unit quaternion $\boldsymbol{\varepsilon} = [\varepsilon_0 \ \bar{\boldsymbol{\varepsilon}}^\top]^\top$ is

$$\boldsymbol{\varepsilon} = \begin{bmatrix} \varepsilon_0 \\ \bar{\boldsymbol{\varepsilon}} \end{bmatrix} = \begin{bmatrix} q_0 & \bar{\mathbf{q}}^\top \\ -\bar{\mathbf{q}} & q_0 \mathbf{I} - \hat{\mathbf{q}} \end{bmatrix} \mathbf{q}^* = \begin{bmatrix} \mathbf{q}^\top \mathbf{q}^* \\ 2E(\mathbf{q})^\top \mathbf{q}^* \end{bmatrix} \quad (33)$$

The target attitude \mathbf{q}^* is one of the two antipodal unit quaternions corresponding to

$$\mathbf{R}(\mathbf{q}^*) = [\boldsymbol{\lambda} \ \boldsymbol{\chi} \times \boldsymbol{\lambda} \ \boldsymbol{\chi}] [-\mathbf{e}_3 \ \mathbf{e}_2 \ \mathbf{e}_1]^\top \quad (34)$$

The value of \mathbf{q}^* is selected so that it varies continuously in time. The target pointing direction is

$$\boldsymbol{\chi} = \frac{(\mathbf{I} - \boldsymbol{\lambda} \boldsymbol{\lambda}^\top) \boldsymbol{\sigma}}{\|(\mathbf{I} - \boldsymbol{\lambda} \boldsymbol{\lambda}^\top) \boldsymbol{\sigma}\|} \quad (35)$$

The dynamic pointing direction is a state of the closed loop system and its evolution is described by the differential equation

$$\begin{aligned} \dot{\boldsymbol{\sigma}} &= k_\eta (\boldsymbol{\sigma} \times \boldsymbol{\lambda}) (\boldsymbol{\sigma} \times \boldsymbol{\lambda})^\top \boldsymbol{\eta} \\ &\quad - k_\lambda (\mathbf{I} - \boldsymbol{\sigma} \boldsymbol{\sigma}^\top) \boldsymbol{\lambda} \left(\frac{\boldsymbol{\sigma}^\top \boldsymbol{\lambda}}{\|\boldsymbol{\sigma} \times \boldsymbol{\lambda}\|} \right) \end{aligned} \quad (36)$$

The commanded pointing direction, $\boldsymbol{\eta}$, is a user-supplied time history. The target thrust direction is

$$\boldsymbol{\lambda} = \mathbf{T}^* / \|\mathbf{T}^*\| \quad (37)$$

The target thrust is

$$\begin{aligned} \mathbf{T}^* &= m \dot{\mathbf{r}}^* - m g \mathbf{e}_3 - \mathbf{R}(\mathbf{q}) \mathbf{a}_f(\mathbf{v}) \\ &\quad + m \left((\mathbf{K}_{11} \mathbf{P}_{11})^2 - \mathbf{P}_{22} \mathbf{P}_{11} \right) \boldsymbol{\xi}_1 \\ &\quad - m (\mathbf{K}_{11} \mathbf{P}_{11} \mathbf{P}_{22} + \mathbf{P}_{22} \mathcal{R}_{22} \mathbf{P}_{22}) \boldsymbol{\xi}_2 \end{aligned} \quad (38)$$

The third error vector is

$$\boldsymbol{\xi}_3 = \bar{\boldsymbol{\varepsilon}} \quad (39)$$

The second error vector is

$$\boldsymbol{\xi}_2 = \frac{1}{m} \mathbf{P}_{22}^{-1} \mathbf{R}(\mathbf{q}) (\mathbf{v} - \underbrace{\mathbf{R}(\mathbf{q})^\top (\dot{\mathbf{r}}^* - \mathbf{K}_{11} \mathbf{P}_{11} \boldsymbol{\xi}_1)}_{=\mathbf{v}^*}) \quad (40)$$

The first error vector is

$$\boldsymbol{\xi}_1 = \mathbf{r} - \mathbf{r}^* \quad (41)$$

The target position, \mathbf{r}^* , is a user-supplied time history.

References

- [1] “Urban Air Mobility (UAM) Concept of Operations,” 2023.
- [2] I. Willebeek-LeMair, S. B. Widman, and C. A. Woolsey, “Input-to-State Stable Energy-Based Position Tracking Control for Atmospheric Flight Vehicles,” in *AIAA SCITECH 2025 Forum*, AIAA, 2025.
- [3] H. Khalil, *Nonlinear Systems*. Pearson Education, Prentice Hall, third ed., 2002.
- [4] J. W. Hopwood, B. M. Simmons, C. A. Woolsey, and J. K. Cooper, “Development and evaluation of multirotor flight dynamic models for estimation and control,” in *AIAA SCITECH 2024 Forum*, AIAA, 2024.
- [5] J. V. Foster and D. Hartman, “High-fidelity multi-rotor unmanned aircraft system (uas) simulation development for trajectory prediction under off-nominal flight dynamics,” in *17th AIAA Aviation Technology, Integration, and Operations Conference*, AIAA, 2017.